Journal of Marine Research, 61, 285–312, 2003

Journal of
MARINE RESEARCH

Volume 61, Number 3

Relative dispersion at the surface of the Gulf of Mexico

by J. H. LaCasce[1,2] and Carter Ohlmann[3]

ABSTRACT

We examine the relative motion of pairs and triplets of surface drifters in the Gulf of Mexico. The mean square pair separations grow exponentially in time from the smallest resolved scale (1 km) to 40–50 km, with an e-folding time of 2–3 days. Thereafter, the dispersion exhibits a power law dependence on time with an exponent of between 2 and 3 (depending on the measure used) up to scales of several hundred kilometers. The straining is for the most part isotropic, with only weak regional variations. But there are suggestions of anisotropy in the western basin, probably due to boundary current advection.

The pair velocities are correlated during the early phase and a portion of the late phase. The relative displacement distributions during the early phase are, after an initial adjustment, non-Gaussian and approximately constant, suggestive of local straining.

The triplet results likewise suggest two growth phases. During the early phase, the mean area and the longest triangle leg grow exponentially in time, the latter with a rate consistent with the two-particle results. Most triangles are drawn out during this time. During the late period, the triangles grow and their aspect ratios systematically decrease, suggesting an evolution to an equilateral shape.

Although surface divergences should affect these statistics, they nevertheless strongly resemble those found with two-dimensional turbulent flows. If so, we would infer an enstrophy cascade at scales below the deformation radius (40–50 km) which is probably spectrally local. The latter implies that growth in particle separations comes from flow features the same size as the separations. It is also possible there is an inverse energy cascade to scales larger than the deformation radius, driven possibly by baroclinic instability. However, the late period statistics may also reflect dispersion by a large scale shear.

1. Woods Hole Oceanographic Institution, Woods Hole, Massachusetts, 02543, U.S.A.
2. Present address: Norwegian Meteorological Institute, P.O. Box 43, Blindern, 0313 Oslo, Norway. ***email: jlacasce@met.no***
3. Institute for Computational Earth System Science, University of California, Santa Barbara, California, 93106, U.S.A.

We do not resolve an upper bound on the late time power law growth (i.e. we do not observe an ultimate diffusive stage). This may reflect shear dispersion. But it may also stem from surface convergences which can cause long time particle correlations, as seen in recent numerical simulations of particles on a surface bounding an interior turbulent flow.

1. Introduction

Lagrangian dispersion concerns the evolution of a marked patch of fluid. The subject has wide-ranging applications, from predicting how oil spills spread and explaining temperature distributions in the ocean, to predicting toxic chemical plume evolution and the ozone distribution in the atmosphere. Generally, one is concerned with the translation and distortion of such a tracer, the former dictating where a cloud goes and the latter how it is mixed into the environment. The mean and variance of tracer concentration can be measured using single particle statistics, whereas the covariance of the concentration requires knowledge of the relative motion of groups of particles. It is the latter which concerns us here.

Many of our theoretical expectations for "relative dispersion" come from turbulence theory. Assuming the existence of a turbulent inertial range, one can deduce how mean square particle separations vary with time and separation, over the range of scales corresponding to the inertial range. We expect, for example, that mean square separations grow as time to the third power in the (energy) inertial range in 3-D turbulence and for the (inverse) energy cascade in 2-D turbulence.[4] In contrast, separations grow *exponentially* in time in the (2-D) enstrophy cascade. Pertinent reviews are given by Bennett (1987) and Babiano *et al.* (1990).

Another relevant area of theory is that of dynamical systems. Broadly speaking this concerns particle motion near specific flow features, often in the context of kinematic models. Pair separations grow linearly in time near elliptic points and exponentially near hyperbolic points; the latter growth is measured in terms of Lyapunov exponents. Boundaries between regions with different mixing characteristics are the stable and unstable "manifolds." There is an extensive literature on the subject, (for example Ottino, 1989). Dynamical systems ideas were used recently in an analysis of drifter data in the Gulf of Mexico by Kuznetsov *et al.* (2002).

The earliest geophysical relative dispersion calculations were made in the atmosphere. Richardson (1926) measured smoke spreading from stacks and showed that the rate of plume growth increased with plume width; that his results were consistent with an energy inertial range was demonstrated by Obhukov (1941) and Batchelor (1952a). In two balloon experiments in the southern hemisphere stratosphere conducted in the 1970's ("EOLE" at 200 mb and "TWERLE" at 150 mb), researchers found evidence for exponential growth at separations of less than 1000 km (Morel and Larcheveque, 1974; Er-el and Peskin, 1981). The behavior at larger scales was less clear; in the EOLE experiment, the mean square pair separations grew linearly in time (as with a

4. The similarity arguments depend on the units of the energy transfer rate, but not on the direction of transfer.

diffusive process) whereas they grew faster than linearly in the TWERLE experiment, and possibly as rapidly as time cubed.

Oceanic observations exist as well. Richardson and Stommel (1948) documented dispersion consistent with an energy cascade at the surface of a pond and the ocean, on scales from 50 cm to 100 m. Okubo (1971), Sullivan (1971) and Anikiev *et al.* (1985) inferred similar behavior from dye spreading at the surface of the ocean (or of a lake) over a large range of scales (see also Bennett, 1987). Davis (1985) and Poulain and Niiler (1989) examined relative dispersion among surface drifters in the California Current and Lacorata *et al.* (2001) did the same for drifters in the Adriatic. These studies did not provide robust evidence of either an exponential or a power law dependence. LaCasce and Bower (2000) examined subsurface floats in the North Atlantic and found inhomogeneous dispersion, with an inverse energy cascade possibly occurring in the west (near the Gulf Stream and the North Atlantic Current), but essentially diffusive spreading in the east.

What remains elusive is observational evidence of exponential stretching in the ocean, as seen in the atmosphere (Morel and Larcheveque, 1974; Er-el and Peskin, 1981). The problem evidently is one of scales. In the atmosphere, the putative enstrophy cascade range extends to 1000 km whereas the energy-containing scale in the ocean is about an order of a magnitude smaller. The minimum separation resolved by LaCasce and Bower (2000) was only about 10 km, or about 5–10 times smaller than the energy containing eddies; this was evidently insufficient to resolve any exponential growth. Brown and Smith (1990) used several techniques to detect exponential growth in SOFAR trajectories but concluded only that the absence of such stretching could not be confirmed. Indirect evidence of such stretching arguably does exist though; the filamentation seen in the tracer release experiments of Ledwell *et al.* (1998) was consistent with exponential stretching (Sundermeyer and Price, 1998). But given the nature of the data, this could not be quantitatively confirmed.

Hereafter we will examine the relative dispersion of surface drifters in the northern Gulf of Mexico. The data set (from the SCULP observational program) possesses much higher drifter densities than in most previous oceanic data sets, offering more instances of closely spaced pairs. It is not uncommon to find pair separations of 1 km here, an order of magnitude smaller than with the subsurface Atlantic float set (LaCasce and Bower, 2000). As such, we are afforded a closer look at pair statistics on scales of 1–50 km. The result is a fairly clear indication of exponential stretching at scales less than about 50 km.[5]

As a point of presentation, we will focus exclusively on the particle group statistics initially. We will defer interpretations (which are necessarily speculative) until the end.

5. While preparing this manuscript, we learned that others may have also detected exponential dispersion, among floats at 1000 m depth in the middle North Atlantic (Colin de Verdiere, pers. comm.).

2. Data

The data come from surface drifters similar in design to those used in the Coastal Ocean Dynamics Experiment (CODE; Davis, 1985). The drifters are composed of four rectangular panels 50 cm wide by 90 cm tall that extend from a vertical tube 10 cm in diameter. Four small surface floats keep the center of the drifter near 0.5 m depth. Technocean Inc. constructed the drifters and packaged them in soluble cardboard boxes with degradable parachutes. The drifters were deployed from aircraft. Once submerged, drifter position within 1000 m was determined 5 to 7 times each day by Doppler ranging of the Argos satellite locating system.

The SCULP field program consisted of 3 distinct segments identified as SCULP I, II, and III (Ohlmann and Niiler, in prep). SCULP-I drifter deployments occurred primarily at 15 stations (distributed as a 3 by 5 grid) within a 125 km square on the Louisiana-Texas shelf. SCULP-I drifter deployments occurred from October, 1993, through July, 1994. The grid was reinitialized weekly for the first three months, then biweekly for three months, and finally monthly, giving roughly one year of data. A total of 389 drifters sampled during the SCULP-I period and drifter half-life was 56 days.

The SCULP-II drifters were deployed within a 400 by 150 km rectangle on the northwest Florida shelf to investigate cross-shore flows. The initial SCULP-II deployment occurred in February, 1996, and consisted of 15 units. The grid was reinitialized every two weeks for roughly a year. A total of 342 drifters sampled during the SCULP-II period and drifter half life was 66 days.

The SCULP-III study was specifically concerned with eddies on the shelf-rise of the Louisiana and North Florida coasts. Four deployments of 20 drifters seeded the edge of warm eddies identified with remotely sensed sea-surface temperature (AVHRR) and SSH (T/P) data. Deployments occurred during April, 1998, on the Louisiana shelf, and during July, 1998, on the continental margin south of the Florida-Louisiana border. The SCULP-III drifters are excluded from this study as they seeded specific flow features and because they only yielded a small number of pairs.

Drifters such as these are advected both by geostrophic and ageostrophic flow near the surface and as such respond to the Ekman drift as well as the large scale flow. Without additional information on how to decompose the velocities, we are forced essentially to ignore the Ekman contribution.[6] The possibility of Ekman advection obviously must be kept in mind when interpreting the results.

Perhaps more critical is that the ocean surface is divergent. Surface drifters must remain at the surface and so cannot follow water parcels that rise or sink. This should in turn cause deviations from theoretical expectations derived for nondivergent flows, such as 2-D turbulence. We will return to this point at the end.

Examples of drifter trajectories are plotted in Figure 1. These are representative of the

6. A reviewer pointed out that the Navy maintains an archive of 10 km resolution winds over the continental US and Central America, and one might use such winds to deduce the Ekman contribution. This is beyond the present scope but suggests an interesting direction for future work.

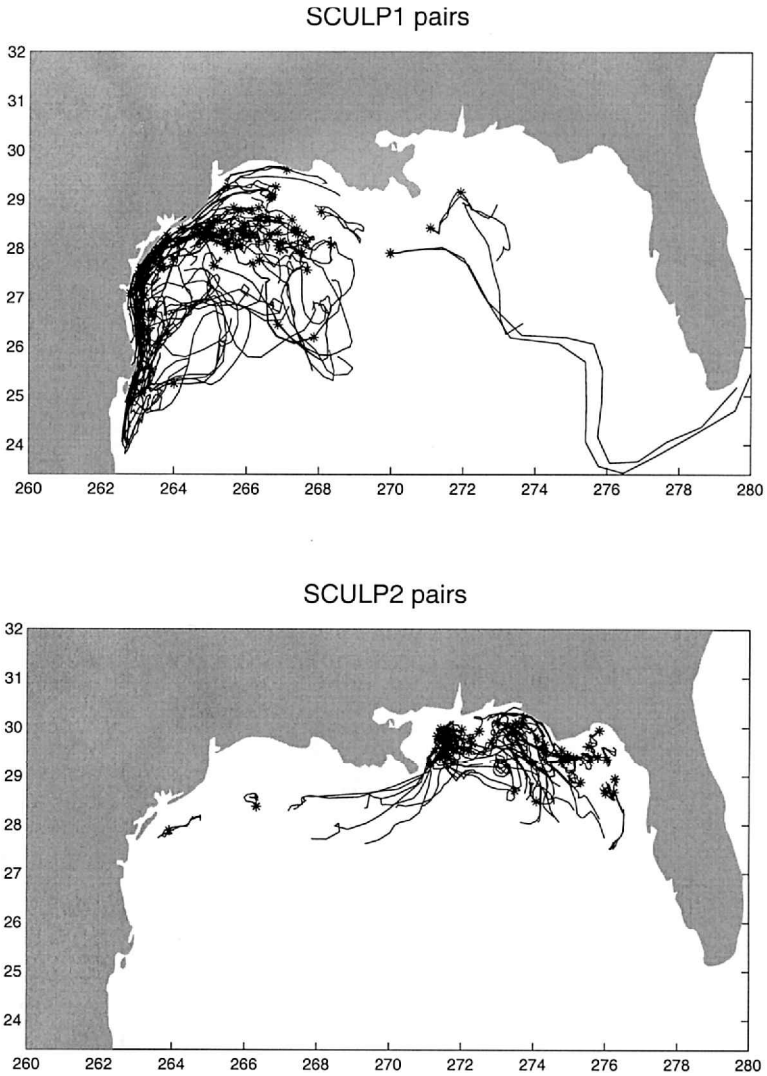

Figure 1. Trajectories of the $r_0 \leq 1$ km pairs of 25 days duration from the SCULP1 and 2 experiments.

pairs used in the calculations (but are only a subset of the whole drifter set). The SCULP1 pairs lie predominantly in the western Gulf and the SCULP2 pairs in the east.

3. Two particle statistics

We will consider two types of statistics hereafter: first those of drifter pairs and then of triplets. To examine how drifter pairs separate as a function of time and space, we will use a

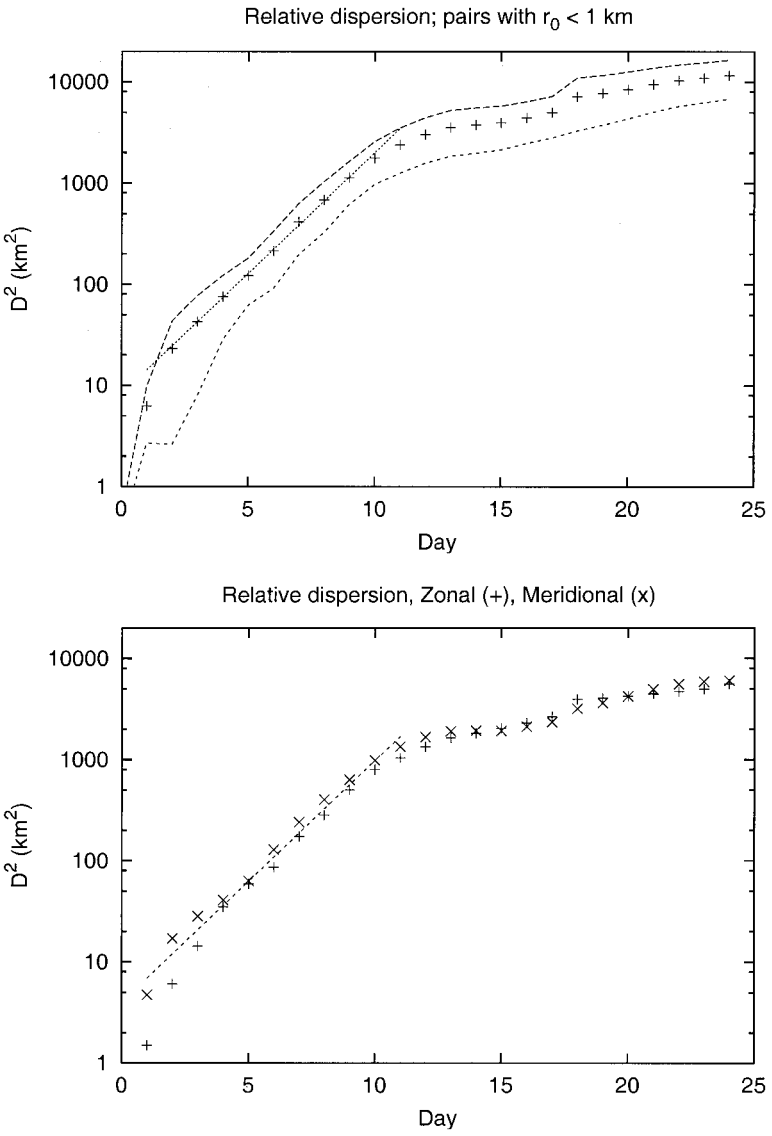

Figure 2. (a) The mean square separation vs. time for the combined SCULP1 and 2 sets. The dashed lines indicate the 95% confidence limits and the straight line represents and exponential growth with a growth rate, determined by least squares, of 0.55. (b) The mean square zonal and meridional separation vs. time for the combined SCULP1 and 2 sets. (c) The mean square separation vs. time for the SCULP1 and 2 sets separately. The dashed lines are the 95% confidence limits for the SCULP1 data.

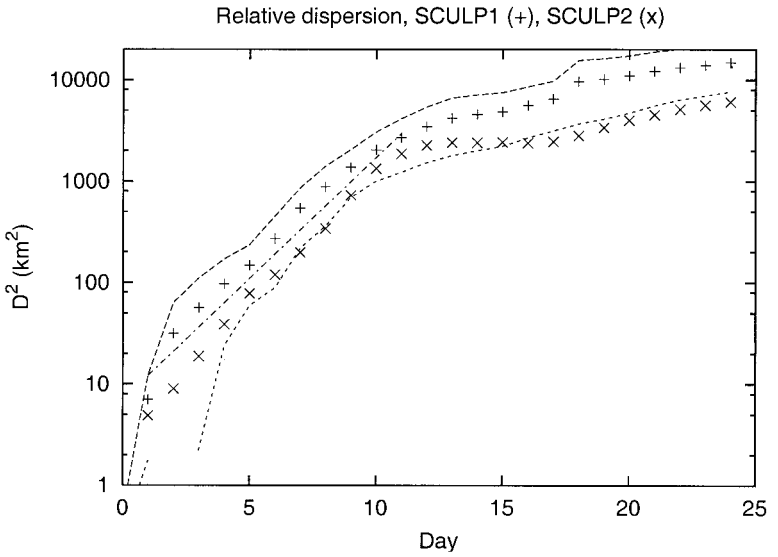

Figure 2. (Continued)

variety of measures deriving from both turbulence and dynamical systems studies; we will introduce them as we go along.

a. Relative dispersion

A commonly used measure of relative dispersion is the mean square pair separation, defined as:

$$D^2(t) \equiv \sum_{i \neq j} (x_i(t) - x_j(t))^2 + (y_i(t) - y_j(t))^2, \tag{1}$$

which indicates how particles separate as a function of time. To calculate this, we select a set of pairs in which the individuals are closer than a given distance, r_0, *at some time.* As in LaCasce and Bower (2000), we include drifters launched together ("original pairs") and those which approach one another later on ("chance pairs"). The majority of our pairs are of the "chance" variety.[7]

The resulting squared separations are then averaged for a fixed period of time (shorter duration trajectories were discarded).[8] There are 140 pair trajectories of 25 days duration with $r_0 \leq 1$ km; these are the trajectories in Figure 1.

7. A potential difficulty is that chance pairs are more likely to have correlated positions and initial velocities, and this can alter the approach to asymptotic dispersion regimes (e.g., Bennett, 1987; Babiano *et al.,* 1990). However, no systematic differences between such "original" and "chance" pairs have been found previously (Morel and Larcheveque, 1974; LaCasce and Bower, 2000). The present set contains too few original pairs to determine whether there is a difference.

8. The averages are typically smoother when one uses such equal length segments. Using 25 day trajectories was a compromise between having a long enough segment to observe the changes and having enough pairs for statistical reliability. However the results do not vary greatly with this choice.

The relative dispersion curve for the $r_0 = 1$ km pairs is shown in Figure 2a on a log-linear scale. We see that the curve at times less than 10 days is approximately linear, and this is our first indication of exponential growth. The best fit exponential has a growth rate of 0.55 ± 0.10, corresponding to an e-folding time is approximately 2 days. Exponential growth occurs over length scales of 5 to 50 km.

The (presumed) exponential growth phase does not begin immediately but is preceded by an adjustment which takes about two days. This may represent a period during which particles lose "memory" of their initial positions and velocities (Bennett, 1987; Babiano *et al.,* 1990). It may also reflect boundary current advection in the west (see below). Its presence however does not imply that exponential growth is absent at scales less than 5 km, merely that we haven't captured that.

Several more points can be deduced. First, the dispersion at all times is isotropic within the errors (Fig. 2b); so there is no preference for either zonal or meridional spreading. This is also true for the SCULP1 and SCULP2 subsets individually.

The second point concerns regional variations. The most important such variation is that pairs in the western Gulf are influenced by a boundary current. The latter flows southwestward along the Gulf coast of Texas, with speeds of several tens of cm/sec in shallower regions. The pair trajectories in this region clearly show the influence of the current (Fig. 1). The current is plainly visible if one box-averages the (single) drifter velocities (Ohlmann and Niiler, in prep.). The pairs most affected are those in the SCULP1 set which begin life inshore of roughly the 50 m isobath; there are 47 such pairs.

With this number of pairs it is impossible to determine their dispersion definitively, but this is evidently closer to a power law growth than an exponential one. If so, the growth rate is somewhat faster than quadratic in time. Such super-diffusive growth can occur with a lateral shear (Sec. 6). Power law growth is initially faster than exponential growth, and it is for this reason that the SCULP1 dispersion is somewhat greater than the SCULP2 dispersion for the first couple of days (Fig. 2c). Notice that the SCULP2 pairs appear to exhibit exponential growth to the smallest resolved scale.

In any case, the boundary pairs evidently have relatively little effect on the early dispersion. This is presumably because they represent a minority of the set of 140, and also perhaps because the power law growth is quickly overshadowed by the exponential one in the mean.

Third, and perhaps most surprising, is that there is no detectable dependence of dispersion on water depth. Many of the drifters originate over the shelf, often in water less than 10 m deep, in both SCULP1 and SCULP2. But excluding pairs which are in such shallow water (at some time) doesn't alter the results. For example, removing all pairs which were in less than 25 m of water reduced the number of pairs from 140 to 75, but did not change the dispersion within the errors. The result is the same excluding those in less than 50 m (although the errors are then significantly larger).[9]

9. One could conceivably look for topographic influences by projecting the dispersion into coordinates parallel and perpendicular to the isobaths. However it is less clear how to do this with relative displacements than with absolute displacements (LaCasce, 2000).

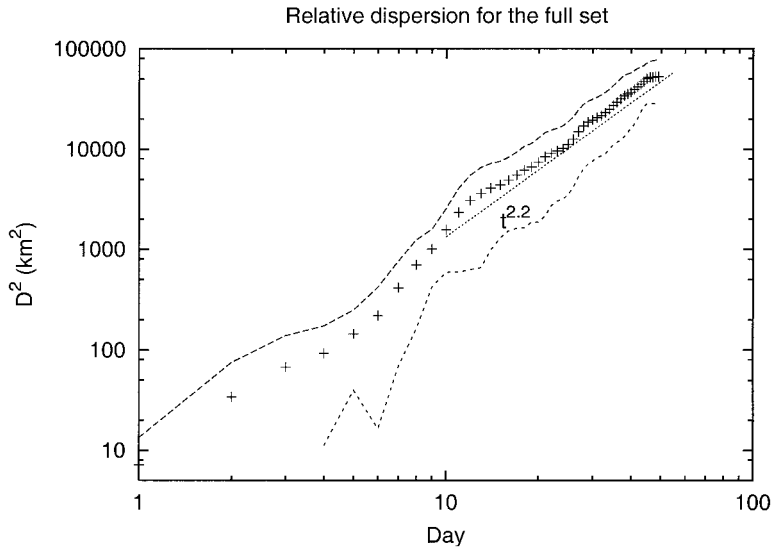

Figure 3. The total dispersion vs. time on a log-log plot (to emphasize the power law growth at later times).

The dispersive growth after day 10 is closer to a power law, as shown in the log-log plot of Figure 3; this curve derives from the smaller set ($n = 65$) of 50 day pair trajectories. The power law dependence is evident from 10 to 50 days, and the best-fit exponent is 2.2 ± 0.8. The meridional dispersion in this period is somewhat greater than the zonal, but not significantly so at the 95% confidence level.

This power law growth is faster than the late time diffusive growth seen in the subsurface North Atlantic, where $D^2 \propto t$ (LaCasce and Bower, 2000). In fact, no such diffusive regime is seen here, at least up to the largest scales sampled (roughly 300 km).

Not shown in the figures are the cross correlations:

$$D_{xy}(t) \equiv \sum_{i \neq j} (x_i - x_j)(y_i - y_j), \tag{2}$$

which are not significantly different from zero for the set as a whole. This is in line with isotropic dispersion. Most of the pairs originate in the northern Gulf, so a zero cross correlation implies no preferred tendency for the pairs to separate westward or eastward. The pairs in the SCULP1 set entrained in the boundary current do have a significant (positive) cross correlation, but this is a biased selection; exclude them and the remaining subset has a negative cross correlation (reflecting southeast-ward motion).

b. Finite time Lyapunov exponents

Our second measure is designed specifically for particles separating exponentially in time. If a pair is separating thus, its maximum Lyapunov exponent (Lichtenberg and Lieberman, 1992):

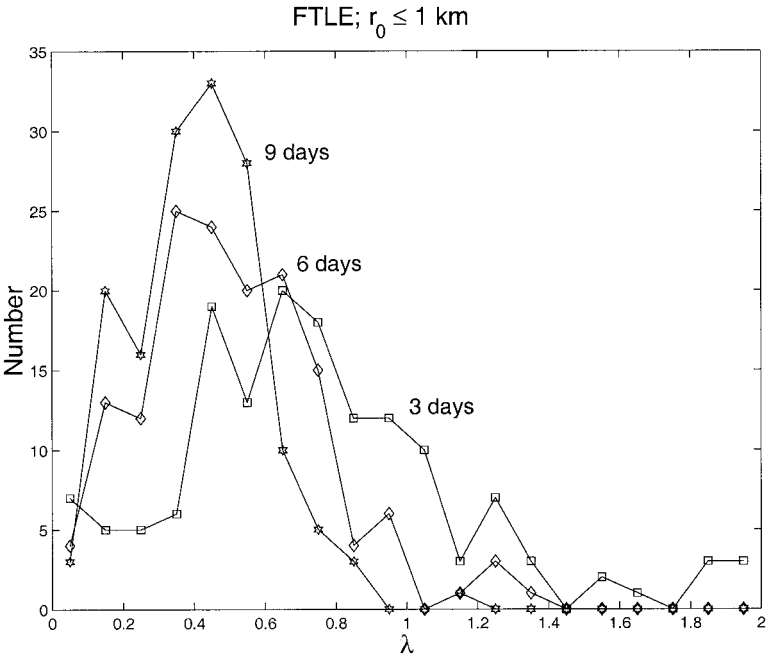

Figure 4. The FTLEs at 3, 6, and 9 days for the $r_0 \leq 1$ km drifter pairs. Note how the distribution becomes narrower in time, with a peak corresponding to an e-folding time of roughly two days.

$$\lambda = \lim_{t\to\infty} \lim_{r(0)\to 0} \frac{1}{t} \log\left(\frac{r(t)}{r(0)}\right) \tag{3}$$

is a nonzero constant (here $r(t)$ and $r(0)$ are the pair separations at times t and 0). However, assuming pairs experience different straining rates over their lifetimes, it makes more sense to calculate the Lyapunov exponent as a function of time, the Finite Time Lyapunov exponent (FTLE):

$$\lambda_T(\tau) = \lim_{r(0)\to 0} \frac{1}{\tau} \log\left(\frac{r(\tau)}{r(0)}\right). \tag{4}$$

One can calculate the FTLE for each pair and then observe the distribution of values as a function of time. To do this, we will use the set of pairs (with $r_0 \leq 1$ km) used previously, excluding those pairs trapped in the western boundary current. Given that the dispersion results imply exponential growth during the first 10 days, we calculated the Lyapunov exponents, $\lambda_T(t)$ during that same period.

Histograms of $\lambda_T(t)$ for days 3, 6 and 9 are shown in Figure 4. The curves suggest distributions which become progressively sharper and whose mean decreases, from 0.77 at $t = 3$, to 0.51 at $t = 6$, to 0.43 at $t = 9$. The corresponding e-folding times thus vary from about one and a half to two and a half days, in agreement with the 2 day time scale deduced from relative dispersion.

The relative sharpness of the distribution suggests that most pairs experience approximately the same straining; broader distributions would mean either more regional or temporal (because the pairs occur at different times) variations. In addition, the distribution of exponents is becoming more Gaussian. The kurtosis[10] decreases from 5.7 at $t = 3$ to 3.4 at $t = 6$ and 3.6 at $t = 9$. Were the flow chaotic, a Gaussian distribution would imply the Lagrangian sampling was *ergodic* (Shepherd *et al.,* 2000), that is, that particles visit all accessible regions. Again, a similar interpretation here is complicated by having pairs at different times.

As a further test for regional variations, we can use the FTLE to partition pairs geographically according to separation rate, for instance by mapping pairs with $0.3 \leq \lambda(t = 9) \leq 0.6$. Doing so however yielded no hints of regional variability; the subsets spanned the same areas as did the larger set.

We emphasize that FTLE's do not prove that exponential stretching is occurring; the present exponents however are consistent with that notion. As stated, the FTLE's also support the previous assertion that the relative dispersion is nearly homogeneous.

c. *Finite scale Lyapunov exponents*

A potential difficulty with relative dispersion as a measure concerns the means of averaging; one averages distances at fixed times. So for example, a pair 10 km apart at day 3 is averaged with another only 1 km apart. If dispersion is dominated by structures the same size as the particle separation, averaging pairs with different separations could blur the dependencies.

An alternate approach is instead to average times at fixed distances. This is the idea behind the so-called "Finite Scale Lyapunov Exponent" or "FSLE" (Aurell *et al.,* 1997; Lacorata *et al.,* 2001; Boffetta and Sokolov, 2002). It is not a new idea; distance is also the independent variable in Richardson's (1926) distance-neighbor formulation (the dependent variable is the time derivative of relative dispersion, the relative diffusivity). But the FSLE has the additional advantage of being effectively an integral quantity rather than a derivative, and so is generally smoother than a diffusivity.

To calculate the FSLE, one chooses a set of distances which increase multiplicatively:

$$R_n = \alpha R_{n-1} = \alpha^n R_0 \tag{5}$$

and then calculates the times required for each pair displacement to grow to successive R_n. The times are then averaged for each distance class. The resulting estimate for the maximum Lyapunov exponent varies with distance and is given by:

$$\lambda_S(n) = \frac{1}{\log(\alpha)} \left\langle \frac{1}{T_n} \right\rangle. \tag{6}$$

10. The kurtosis is the fourth order moment normalized by the squared second order moment. For a Gaussian distribution, it has a value of three.

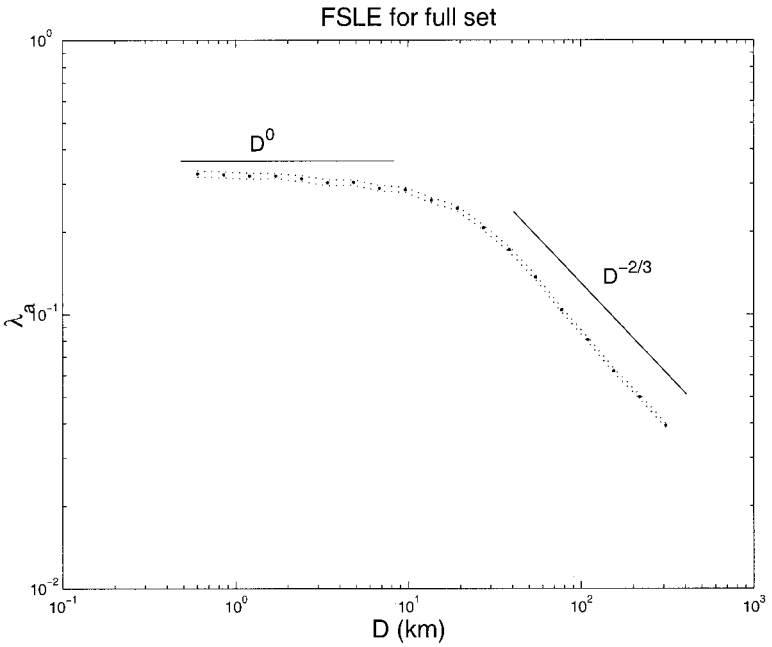

Figure 5. The FSLEs for the full data set. The small dotted lines indicate the 95% confidence limits. The implied Lyapunov exponent is nearly constant at small scales, and decays as $D^{2/3}$ at larger scales.

An important difference with the FSLE concerns which pairs are used. Whereas the previous measures used the subset of "chance" and "original" pairs closer than a certain separation (r_0) at one time, the FSLE uses *all* sets of possible pairs. We record the separation as a function of time for each pair of drifters (present at the same time), from the minimum separation to the final separation at the end of the pair's lifetime. The times required to move from one distance marker, R_n, to the next are found and added to the relevant bins. The means thus represent different numbers of pairs, with larger numbers at larger separations.

We used all the drifters for this calculation, including those initially in the boundary current in the west (using only the SCULP1 or SCULP2 data yielded essentially the same results). We chose the scale factor in (5) to be $\alpha = \sqrt{2}$ (an arbitrary choice which merely determines the number of bins). The result for the full set of data is shown in Figure 5. Plotted is the Lyapunov exponent, $\lambda_S(r)$, vs. distance; also shown are the estimated 95% confidence limits (which are narrow due to the very large number of pairs).

Like the relative dispersion, the FSLE suggests two phases of growth. At scales smaller than about 10–20 km (early times), λ_S is nearly constant; at larger distances, it is decreasing with an approximate power law dependence on distance.

Consider the early phase. The Lyapunov exponent at small scales is decreasing, but very slowly. Were it constant, it would imply exponential growth because the associated

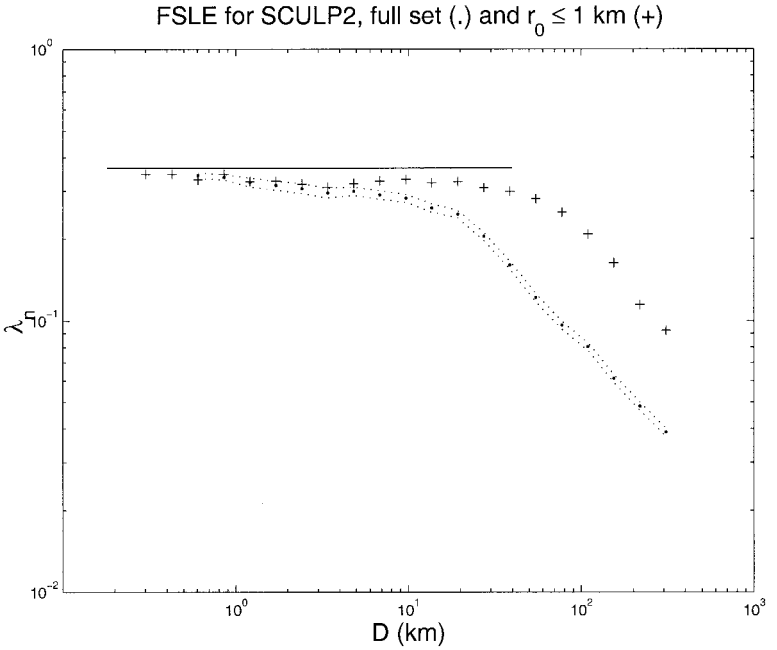

Figure 6. The FSLEs for the SCULP2 set and for the subset of SCULP2 drifters which have $r_0 \leq$ 1 km. The Lyapunov exponent is nearly constant over a larger range of scales in the subset.

e-folding time would likewise be constant. The Lyapunov exponent here is roughly 0.35, corresponding to an e-folding time of about three days. The curve suggests it is constant up to a scale of 10 km.

Recall that relative dispersion suggested an e-folding of 2 days and exponential growth up to roughly 50 km. The difference in time scales is not large but the discrepancy in length scales is harder to ignore. There are two possible causes for the latter: the use of all available pairs in the FSLE and/or the change in dependent and independent variables.

To infer which is more important, we calculated the FSLE for two sets, the full set of SCULP2 pairs and those with $r_0 \leq 1$ km initially (as noted, the dispersion for the SCULP2 set is identical to that of the combined set). We see (Fig. 6) that the subset has a constant Lyapunov exponent which is about the same as that calculated for the full set. But now the near-exponential growth persists to 40–50 km. So the earlier decrease in λ_n for the FSLE from the full set of pairs is due to having more pairs.

Why would this be? Flow inhomogeneity is one possible explanation; if so, it is by chance that the drifters with $r_0 \leq 1$ km happen to lie in regions where there is exponential growth up to 50 km. The drifters with $1 < r_0 < 10$ km lie in regions where such growth occurs only up to 10 km. Such a situation obviously seems fortuitous (and our previous indications suggest to the contrary that the straining is largely homogeneous in the sampled regions).

A more likely possibility is that the drifters with $1 < r_0 < 10$ km still have correlations

between their positions and velocities, delaying the onset of exponential growth. This effect is clearly seen in numerical experiments (Babiano *et al.,* 1990). It is also a likely reason why LaCasce and Bower (2000) never observed exponential growth: their floats were too far apart initially. It is not known what causes the correlations for these pairs, but this may stem from using "chance" rather than original pairs; we cannot evaluate this without more data.

As noted, the $r_0 \leq 1$ km subset and the full set have identical e-folding times (Fig. 6). So the difference in growth rate from that predicted by relative dispersion stems from the change in independent variable, not the addition of more pairs. This difference is however small; so the variable change at least with this set is of secondary importance. Indeed the general agreement between Figures 6 and 2 at small scales suggest the relative dispersion and the FSLE are in quantitative agreement.

Then there is the decrease of the FSLE at large scales. Like the relative dispersion, the FSLE suggests a power law dependence. But here $\langle 1/T \rangle \propto D^{-2/3}$, implying the mean square distance is growing as time *cubed.* This is not significantly different than the result from relative dispersion, given the errors on the latter. In fact, the exponent is better constrained with the FSLE because the latter uses all pairs available at a given time, regardless of their nearest separation. Where the relative dispersion calculation used 65 pairs of 50 days duration, the FSLE has 7280 pairs with separations of 75 km. The number of pairs with larger separations is greater still. Note too that the FSLE calculated for the subset of drifters with $r_0 \leq 1$ km also exhibits a $D^{-2/3}$ decay at large scales (Fig. 6) (here again the FSLE has more pairs at large separations).

Lastly, the FSLE, like the relative dispersion, does not change at the largest sampled scales. In other words, the power law growth evidently increases without bound. We know this cannot be, because eventually the coasts will limit separations (as seen in the Adriatic by Lacorata *et al.,* 2001). However the Gulf is more than 1000 km across, a scale substantially larger than our largest pair separations, so the drifter lifetimes are evidently too short for us to resolve growth saturation.

The FSLE therefore supports exponential growth in pair separations at scales less than 40–50 km, with a e-folding time of roughly 3 days. To capture properly the upper bound on this growth, we had to restrict the set to pairs with $r_0 \leq 1$ km. The implied growth at large scales, such that $D^2 \propto t^3$, is faster than that deduced from relative dispersion. The difference comes apparently from the FSLE averaging over many more pairs.

d. Relative velocities and displacements

A signature of processes like chaotic advection is that the pair velocities are correlated. In contrast, particles experiencing a random walk have uncorrelated velocities, with an rms two particle velocity difference just twice the single particle rms velocity:

$$\langle (u_i - u_j)^2 \rangle = \langle (u_i)^2 \rangle + \langle (u_j)^2 \rangle - 2\langle u_i u_j \rangle \approx 2\langle (u_i)^2 \rangle. \tag{7}$$

The ratio of the relative velocity variance to twice the single particle velocity variance is thus a useful measure of pair velocity correlation (e.g. LaCasce and Bower, 2000). Using

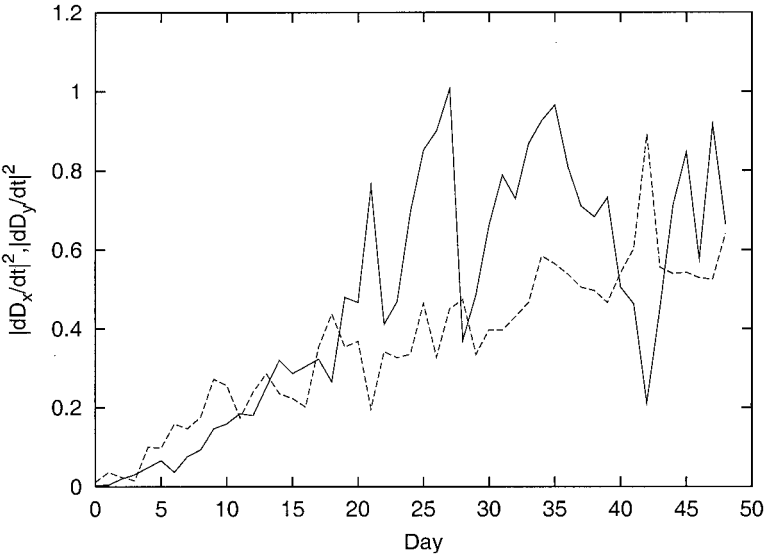

Figure 7. The relative velocity variances in the zonal (solid) and meridional (dashed) directions as functions of time. The variances have been normalized by twice the single particle variance, so that decorrelated pair velocities would have a normalized variance of one.

the $r_0 \leq 1$ km pairs of 50 days duration, we see that the drifter velocities are correlated over at least the first 25 days (Fig. 7). Thereafter the normalized variance fluctuates (and possibly increases in the meridional direction) around a value somewhat less than one.

We see that the early period of exponential growth is also one of correlated pair velocities. The late period dispersion is super-diffusive (D^2 increases faster than linearly in time) and the variances suggest correlated velocities at this time as well. The super-diffusive dispersion persists at least to day 50; the variances may or may not be increasing after day 25, but still may be less than unity at the latest times.

We may compare these variances to those found by LaCasce and Bower (2000) for subsurface floats in the North Atlantic. In the eastern Atlantic, their (normalized) variances were near one for the entire period, suggesting pair velocities essentially uncorrelated from the outset (the minimum separation, r_0, was roughly 10 km). In the west though the variances were similar to these: small initially and rising to a value near one after roughly 30 days. So there, as here, we inferred correlated velocities over at least the initial period.

One can also examine how velocity correlations vary with pair separation. Theoretical arguments suggest that if (under certain circumstances) relative dispersion has a particular dependence on time, then the relative velocity variance should exhibit a dependence on the separation distance. With exponential dispersion for instance, the mean square relative velocity should be proportional to distance squared (e.g. Morel and Larcheveque, 1974). We evaluated this dependency in two ways, first by comparing the variances at fixed times vs. the root of the dispersion at the same times and second, by binning the variances in distance bins, as with the FSLE. The results however were not consistent, even in the early

period. It is unclear why this was so, although it may be the relative velocities, involving differences, converge more slowly than the dispersion.[11]

Lastly we consider the distribution of relative displacements. The probability density function (PDF) of displacements is of central importance because all moments are derived from it (relative dispersion being the second moment). Particles undergoing a random walk would have a Gaussian displacement PDF, with a kurtosis of three. But coherent advection often produces non-Gaussian PDFs; previous observations suggest the latter may be common. Er-el and Peskin (1981) found non-Gaussian PDFs for both zonal and meridional separations between balloon pairs from the TWERLE experiment, at a point during an exponential growth phase. Davis (1985) found the distribution of displacements between drifter pairs in the CODE set off California were non-Gaussian at times soon after deployment. And LaCasce and Bower (2000) found non-Gaussian PDFs among float pairs in the subsurface western North Atlantic, during a super-diffusive growth phase. In all cases, the PDFs had elevated kurtoses, indicating an excess of large (energetic) displacements over what one would have with a Gaussian distribution.

Here too theory provides predictions (discussed hereafter). Of interest at the moment is whether the PDFs *change* in time. Er-el and Peskin (1981) calculated the displacement kurtosis at only one time, so we don't know whether their PDFs were evolving or not. Davis (1985) calculated the PDFs at two times, once after deployment, when the PDF was non-Gaussian, and later when it was Gaussian. But we don't know whether the kurtosis changed during the early period. LaCasce and Bower did monitor the PDFs in time and their kurtoses (in the western Atlantic) were evidently fluctuating around a constant value.

The relative displacement kurtoses from the SCULP data are shown in Figure 8; plotted are the zonal, meridional and total displacement kurtoses. There are several interesting features. All three kurtoses are elevated during the first 20–25 days. But the meridional kurtosis exhibits a sharp increase in the first two days which is not mirrored in the zonal kurtosis. From days 5 to 25, the kurtoses are comparable in both directions and are hovering around a constant value (although noisy). After day 25, the zonal kurtosis is approximately three but the meridional kurtosis remains elevated; the latter causes the total displacement kurtosis also to be somewhat greater than three at late times.

The rapid initial growth in the meridional kurtosis may reflect the influence of the boundary current, because the latter is meridionally-oriented where most of the pairs are (Fig. 1). The meridional growth moreover is found with the SCULP1 set but not the SCULP2 set.

But the initial anisotropy is evidently a transient and, as stated, the kurtoses in both directions are comparable, non-Gaussian and approximately constant from day 5 to nearly day 25. The total kurtosis hovers around a value of 7, exactly as it did with the western

11. Morel and Larcheveque (1974), in studying the EOLE ballon pairs, observed exponential growth up to scales of about 1000 km, as noted previously. Their velocity variances however exhibited a dependence on distance which was not consistent with the dispersion. Curiously, the observed dependence (deduced from their Fig. 9) was similar to ours using the first method of calculation. This agreement is perhaps fortuitous.

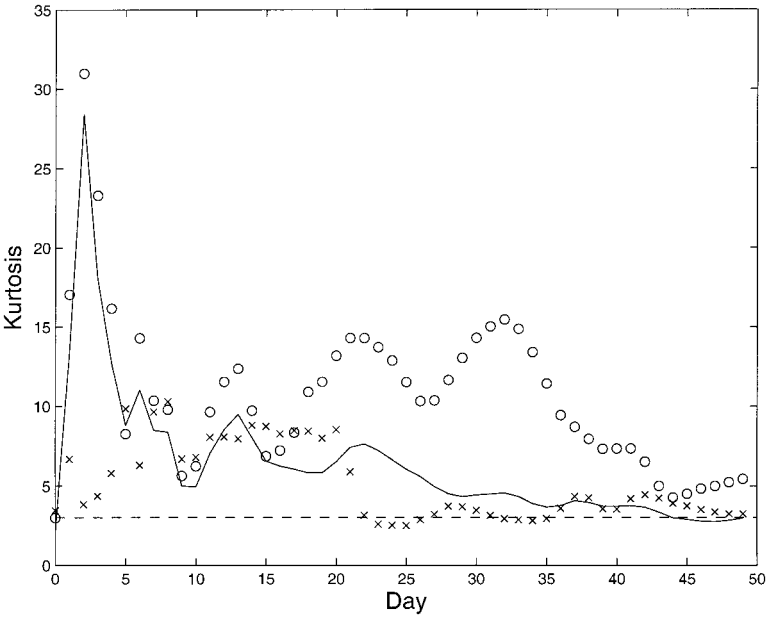

Figure 8. The kurtosis of the relative displacements as functions of time. The solid line is for the total displacements and the circles/crosses are for the meridional/zonal displacements. Note the former is not simply the mean of the latter two. A value of three, indicating a Gaussian distribution, is indicated.

Atlantic float data of LaCasce and Bower (2000). After the initial adjustment, the PDFs thus maintain their shapes, approximately.

The late time behavior is also of interest. We noted earlier that the late time dispersion was isotropic at the 95% level. But this is not in conflict with having anisotropic kurtoses because the latter, being a fourth order moment, is more sensitive to outliers. The discrepancy is more pronounced in the SCULP1 set, so the cause of the anisotropy is in the west and is likely the boundary current. While only a minority of the pairs are in the current, the number is large enough to affect the kurtoses, evidently.

To summarize, the relative velocities and displacements are consistent with correlated pair velocities during the first 25 days (and possibly longer). The relative displacement kurtoses are approximately constant during this early period, following transient growth which only occurs in the meridional direction. After day 25, the zonal kurtosis is Gaussian but the meridional kurtosis is not. These anisotropies may stem from boundary current advection in the west.

4. Three particle dispersion

Given the relatively large number of drifters in this data set, we can go beyond two particle statistics to consider the behavior of clusters. Surface drifter clusters have been

examined before by Okubo and Ebbesmeyer (1976) and Molinari and Kirwan (1975). These authors discussed in particular how to deduce vorticity, divergence and strain rates from the group displacements. But where their focus was single clusters, we will consider instead the average behavior of a number of different clusters.

The theory pertaining to clusters of particles dates back at least to Batchelor (1952b). He considered what would happen to a fluid patch small enough so that the local strain field was approximately uniform (as in the dissipation range in 3-D turbulence). The patch would be flattened out as it spread exponentially in two directions and collapsed exponentially in the third (that the latter balances the former is required by incompressibility). The prediction was consistent with observations of dispersing heat anomalies in the laboratory (Townsend, 1951).

More recently, particle clusters have been examined in light of their relation to multi-point Eulerian correlations of tracer concentration (in particular, the so-called "scalar turbulence" problem). Pertinent reviews are given by Warhaft (2000), Shraiman and Siggia (2000) and Falkovich *et al.* (2001). Multi-point correlations can reveal aspects of the mixing geometry which two point correlations are unable to resolve, and this has direct consequences for clusters of particles (Pumir, 1998; Celani and Vergassola, 2001).

Hereafter we examine triangles of drifters. We searched for triangles in the SCULP data set in much the same way that we sought pairs (in other words, we use "chance" triangles). We found pairs which shared a single drifter, then checked the closest all three were at a given time. If the sum of the two pair distances was less than a certain amount (say, 2 km), then we selected that triangle. As before, we chose equal length records for averaging. As with the two particle statistics, the triplets appear to exhibit two evolutionary phases. We consider each in turn.

a. Early period

The early growth period coincides with the exponential growth phase for the particle pairs (the first 10 days). Were the ocean surface incompressible, then exponential growth in one direction would be balanced by exponential contraction in the normal direction, as in Batchelor's theory. Patches would be drawn out into filaments. Of course the sea surface is not non-divergent, but this is a useful conceptual reference.

For this period, we used 15 day triangle trajectories, derived from the $r_0 \leq 1$ km pairs; we extracted 32 triangles of this duration with the two leg separation of 2 km.[12] A typical trajectory is shown in Figure 9. The triangle translates and rotates, stretching as it goes. However it is clear that the area is increasing in time. This is true in the mean as well (Fig. 10). The area is growing exponentially during the first 10 days, with an e-folding time comparable to that inferred from two particle relative dispersion (about 2 days; Sec. 3a).

A triangle can be characterized by two normal distances, its base and its height. To be definite, we define the base to be the longest triangle leg; the height is then twice the area

12. Some triangles shared two drifters, meaning the 32 realizations are not statistically independent. So the error bars on the following plots should be regarded as a lower bound on the 95% confidence interval.

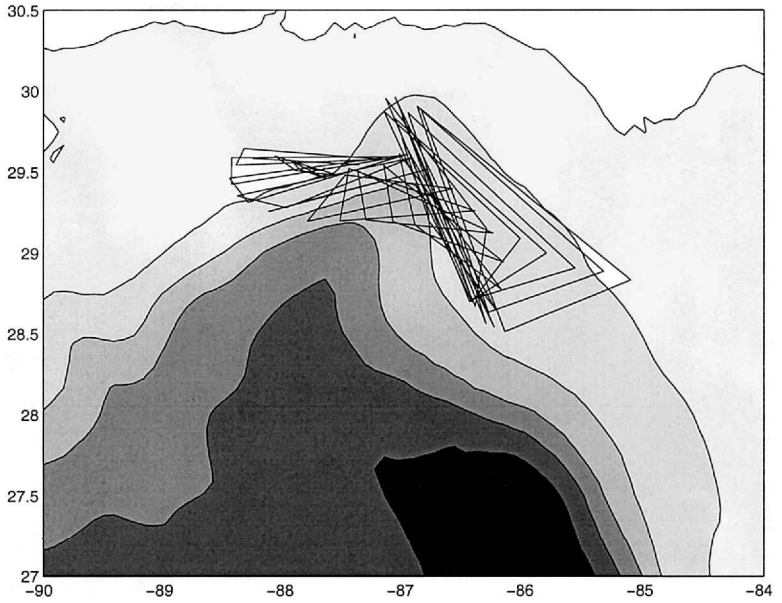

Figure 9. The trajectory of a triangle of drifters over a 25 day period. The sum of the three sides is less than 3 km initially. The trajectory is superimposed on smoothed contours of the bottom topography; shown are the 0, 100, 500, 1000, 2000 and 3000 m isobaths.

divided by the base. We see (Fig. 11) that the mean triangle base is growing exponentially during the first 10 days, with a e-folding rate of 0.28. This corresponds to a time scale about two days for the dispersion (a squared distance). So the base pairs are behaving like the larger set of pairs considered in Section 3a.

However, the mean height is also growing. If the height were actually contracting, we would expect to see it hover around 1 km, the spatial resolution of the data. But while it is near 1 km for the first week, but is significantly greater than that by day 9. Of course, this is near the end of the exponential growth phase, when the triangle area is probably no longer representative of a true 2-D marked fluid, but there nevertheless seems to be monotonic growth during the early period. We cannot say with certainty whether this growth is exponential or something else (for instance a power law dependence).

As noted, surface divergence is a possible cause for the areal growth. To check this, we used the triplets to calculate vorticity and divergence, following the prescription of Okubo and Ebbesmeyer (1976) and Molinari and Kirwan (1975). This method assumes the cluster is small enough so that the shears are locally linear (i.e. it retains the first order terms in a Taylor expansion of the velocity relative to the cluster center of mass).[13]

13. The second order terms are assumed to be due to noise. One then minimizes the noise in a least squares sense to obtain estimates of the velocity shears at the cluster center. A triangle represents the smallest cluster one can use; then the residual of the fit (the noise estimate) is identically zero. Okubo and Ebbesmeyer suggest using at least 6 particles, but this was not possible with the present data.

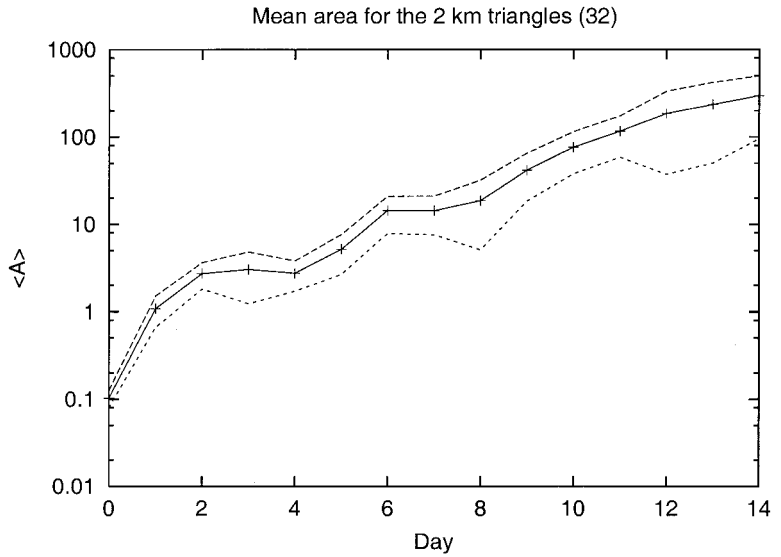

Figure 10. The mean area of 32 triangles found from pairs less than 1 km apart. The error bars are the 95% confidence limits for a student *t* distribution with 31 degrees of freedom. As stated in the text, the actual number of degrees of freedom is probably smaller, given that some triangles share two drifters.

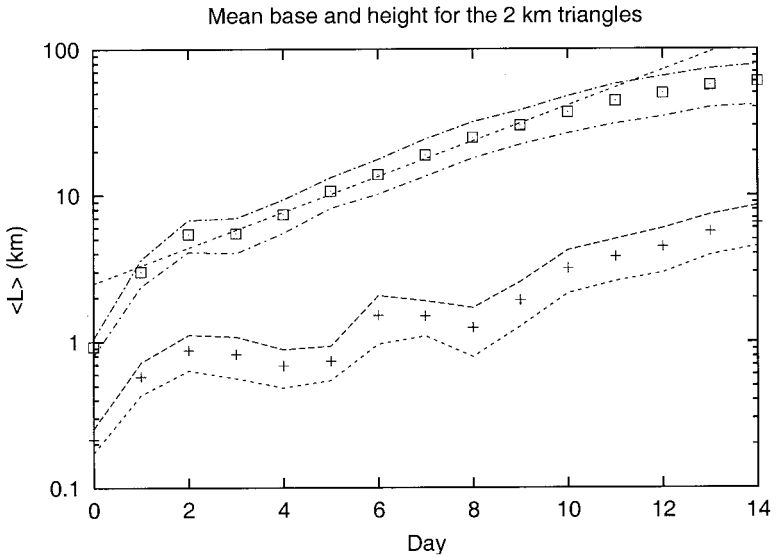

Figure 11. The mean base (squares) and height (pluses) of the 32 triangles from the 1 km pairs. The straight line represents a best-fit exponential with a growth rate of 0.28.

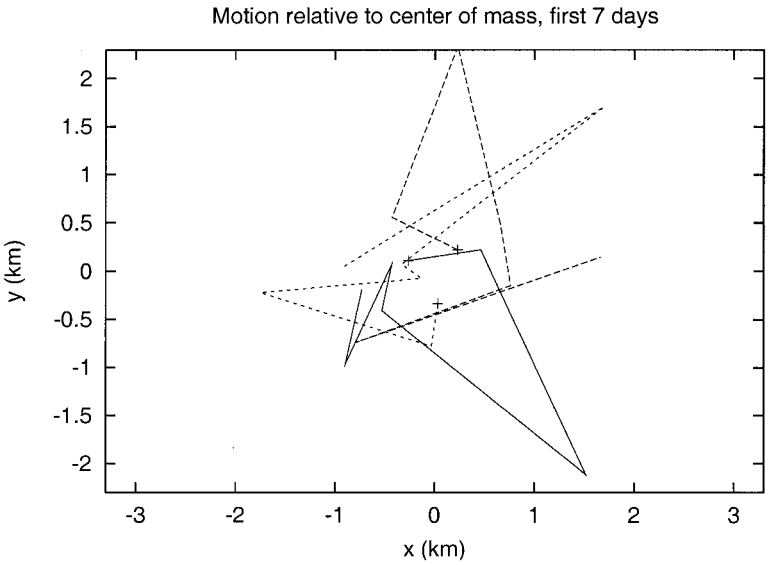

Figure 12. The positions of three drifters relative to their center of mass, during the initial week of the triangle lifetime. Note the apparently random motion, with scales on the order of 1 km.

Performing the calculation and then averaging among the triangles, we found the estimated rms divergence and vorticity were of the same order, roughly 5×10^{-5} sec^{-1}, and did not vary in time. The mean divergence and vorticity were not different from zero at the 95% level. Such estimates by themselves are not unrealistic, but the calculated time series of vorticity and divergence exhibited large changes from day to day, and frequently even changed sign. Similar behavior was found for individual drifter clusters by Molinari and Kirwan (1975).

To understand these changes, we examined the individual drifters' motion relative to the center of mass in different triangles. A typical example is shown in Figure 12 from the period during the first 7 days. Despite that the triangle as a whole moves smoothly, as in Figure 9, the drifters' motions relative to the center of mass are quite random, with each drifter making sudden 1–2 km jumps in different directions. These jumps will obviously corrupt shear estimates, yielding the sudden sign changes mentioned before. Moreover adding a fourth or fifth drifter (assuming similarly random jumps) is unlikely to improve the situation much.

There are several possible explanations for the random jumps. There is the aforementioned satellite positioning error of about 1 km. Then there is the surface Ekman flow, which we have ignored but which could also cause deflections from large scale advective patterns. And then there is the fact that drifters "slip" in the wind; a typical error associated with windage is 1 cm/sec for a 10 m/sec wind, so daily changes in wind could produce 1 km deflections. So there are several plausible explanations.

These random jumps may be the cause of the apparent growth in the mean triangle

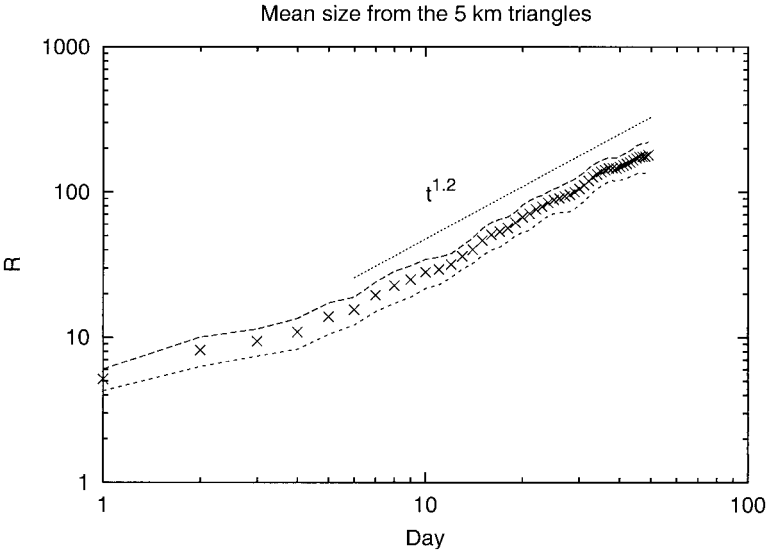

Figure 13. The mean size R (the rms of the triangle legs) of triangles derived from pairs with $r_0 \leq$ 5 km. The 95% confidence limits are shown, as is a power law growth of $t^{1.2}$.

height, as discussed hereafter. Future studies with higher resolution drifter data (say with drifters tracked by the Global Positioning System) may help elucidate this issue.

b. Late period

Beyond 10 days, the drifter triangles presumably no longer reflect a patch of fluid (they also contain "unmarked fluid") and their areas will change. The two particle results for this time period suggest that squared distances between drifters grow as a power law of time. So we would expect, for instance, the rms of the triangle leg distances:

$$R^2 \equiv \frac{1}{3}\,(r_{12}^2 + r_{23}^2 + r_{13}^2)$$

should grow similarly.

To examine this, we require data from a longer period. Since there are only 5 triangles from the $r_0 \leq 1$ km pairs which last for 50 days, we must take larger initial separations. Using instead the $r_0 \leq 5$ km pairs, we increase the set to (a still modest) $N = 25$. Their mean rms leg, R, is shown in Figure 13. It exhibits a power law growth from just before day 10 to day 50, from scales of roughly 20 km to 200 km. The best fit exponent is 1.2 ± 0.2, corresponding to mean square separations growing like $t^{2.4 \pm 0.4}$. This is consistent with the relative dispersion result (where $D^2 \propto t^{2.2}$).

The point of interest here, with regards to theory, is that the triangle *shape* should change to accommodate its growth in size, a consequence of Lagrangian particles maintaining a constant tracer correlation (Celani and Vergassola, 2001). Theory predicts that triangles

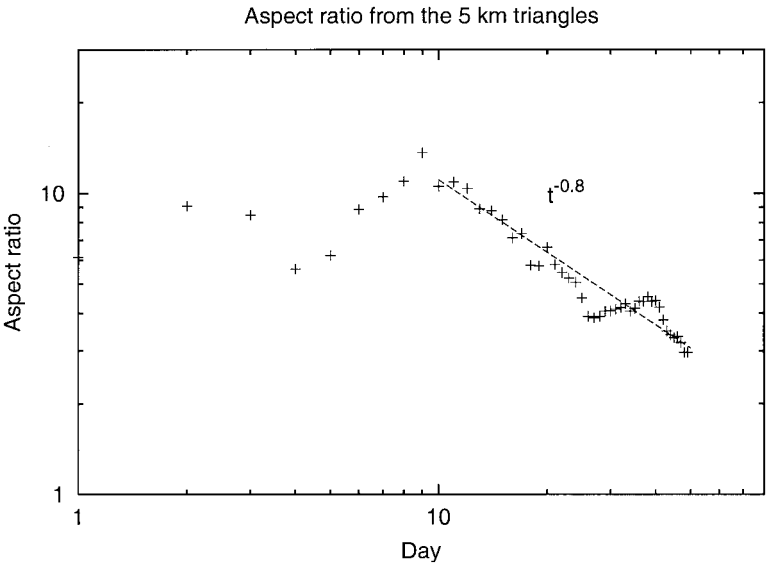

Figure 14. The mean aspect ratio (base divided by height) of triangles derived from pairs with $r_0 \leq$ 5 km. The aspect ratio during the late period decreases approximately as $t^{-4/5}$.

which are "degenerate" (have all three vertices on the same line) evolve toward an equilateral shape in a Richardson growth regime ($D^2 \propto t^3$).

We observe such changes. Exponential stretching during the early period leave the triangles in something close to a degenerate state (as in a filament), but thereafter the triangles become more equilateral. We can gauge this by tracking the ratio of the mean triangle base to the mean height (Fig. 14). The aspect ratio is large during the initial period, with the base roughly an order of magnitude larger than the height. But during the late phase, after day 10, the aspect ratio decreases monotonically. In fact, the ratio decreases approximately as $t^{-4/5}$ to day 50. Obviously this power law decrease cannot continue indefinitely, if the triplets evolve to equilateral triangles (with nearly unitary aspect ratio). But the trend is clear.

5. Summary

We have examined the statistics of pairs and triplets of surface drifters in the Gulf of Mexico. The two particle statistics suggest two growth phases: an approximately exponential growth up to 40–50 km separations, with an e-folding time of 2–3 days, followed by a power law growth to larger scales. No diffusive regime was seen, at least up to the largest sampled scales (roughly 300 km). The different measures used agree on the exponential growth, but predict slightly different growth rates in the late period; relative dispersion suggests $D^2 \propto t^{2.2}$ whereas the FSLE implies growth which is cubic in time. The two particle relative velocities are correlated during the early phase and at least a portion of the

late phase. During the early phase, the relative displacements have roughly constant kurtoses.

The measures for the most part suggest isotropic straining with at best weak regional variations. However, there are several indications of anisotropy in the western basin, in the early dispersion and more particularly in the displacement kurtosis (which is more sensitive to outliers in the distribution). The likely cause is the swift southward-flowing boundary current there, which advects a number of the pairs.

The three particle statistics also suggest two growth phases. During the initial phase, the mean triangle area and its longest leg are growing exponentially in time with e-folding times consistent with that deduced from two particle dispersion. During the late phase, the rms triangle leg exhibits a power law growth with $R \propto t^{1.2}$. This corresponds to a dispersive growth proportional to $t^{2.4}$, comparable to that inferred from two particle dispersion. At the same time, the mean triangle aspect ratio (defined as the ratio of the triangle base, the longest leg, to its height) decreases monotonically.

6. Discussion

The present results bear similarities to those found in two dimensional turbulence. The 2-D enstrophy cascade has exponential growth in pair separations (Bennett, 1987; Babiano *et al.,* 1990), as seen here at small scales. If this is occurring, we would infer a source of enstrophy at the 40–50 km scale and an enstrophy cascade to smaller scales.

Exponential growth could occur with either a collection of 50 km eddies (a "nonlocal" cascade) or with a continuum of eddy scales (a local cascade). However, in the former case, the relative displacement kurtoses would be expected to grow exponentially; in a local cascade, the kurtoses are constant (Bennett, 1984). The present kurtoses were approximately constant at small scales, so the cascade is at most weakly non-local (corresponding to a κ^{-3} wavenumber spectrum of kinetic energy).

The 2-D turbulent energy cascade exhibits pair dispersion which increases cubically in time, as may be the case here at large scales. If so, we would infer a source of energy at 40–50 km. The most likely candidate is baroclinic instability, given that the deformation radius in the Gulf is roughly 45 km (Chelton *et al.,* 1998). The energy cascade moreover is thought to be a local phenomenon, so we would not expect to see increasing displacement kurtoses here either.

Contrary to as assumed in 2-D turbulence though, the ocean surface is divergent. Interestingly, turbulent dispersion in compressible flows has been examined recently (Falkovich *et al.,* 2001 and references therein). An example of the system studied is a rigid surface bounding a volume which is experiencing isotropic, homogeneous 3-D turbulence. Schumacher and Eckhardt (2002) have examined relative dispersion in such an environment, and they find that pairs on the surface exhibit Richardson dispersion (as would be expected for pairs in the interior). Interestingly, they also observe that the pairs *never* reach a diffusive stage; this they attribute to long term particle correlations induced by convergent clustering.

We must be cautious in making direct comparisons because the ocean interior is

different than in the aforementioned models. In particular, the interior flow at scales greater than a kilometer is closer to two dimensional, with the vertical velocity second order. Given that, surface divergences may be less important than with a fully 3-D interior flow, and if so, the surface relative dispersion might mirror the quasi-2-D dispersion in the interior. Obviously we would have to characterize the subsurface dispersion in the Gulf to substantiate such a claim. But the most intriguing similarity is that we likewise do not observe a late-time diffusive stage, and this is perhaps related to surface convergences.

Recall that LaCasce and Bower (2000) observed dispersion consistent with an inverse cascade from scales of roughly 10 to 200 km, near the Gulf Stream. But they also observed diffusive spreading at the largest scales (greater than 200 km). The difference may be that their study employed subsurface floats which are less subject to divergence effects.

However, the large scale dispersion can also possibly be explained by stochastic mixing in the presence of a lateral shear (e.g. Bennett, 1987). Consider a linearly-sheared zonal flow with isotropic stochastic (random) motion superimposed. The pair displacements would obey:

$$\Delta y \propto t^{1/2},\ \Delta x \propto t^{1/2} + U(y)t \ \rightarrow\ \Delta x \propto t^{3/2} + O|t^{1/2}|, \tag{8}$$

and the zonal dispersion would hence increase cubically in time. We have several indications of lateral shear. For one, we see that pairs in the western Gulf are advected by a boundary current (Fig. 1). Second, the SCULP1 relative dispersion increases faster than the SCULP2 dispersion initially, perhaps with a power law growth. Lastly, the displacement kurtoses are anisotropic in the late phase, with non-Gaussian displacements only in the meridional direction (Fig. 8). Shear dispersion could also prevent late-time diffusion.

But there are objections to the shear explanation as well. For one, it would be only by coincidence that shear dispersion begins at the deformation radius. Why wouldn't the transition from exponential growth occur at a larger scale? Second, a linear shear should draw triangles of particles out; in the example above, the aspect ratio of the longest leg divided by the height should *increase* linearly in time. Our three particle statistics indicate the opposite occurs. The only way to explain our results would be if the early exponential growth was occurring perpendicular to the shear, which seems unlikely.

However, given the different indications, we believe that neither shear dispersion nor an inverse cascade can rigorously be ruled out. And of course, both might be occurring simultaneously.

A reviewer pointed out that the present results, regardless of any association with 2-D turbulence, are probably still indicative of the Eulerian energetics. As discussed by Bennett (1987) and Babiano *et al.* (1990), relative dispersion can be used to deduce the wavenumber spectrum of the kinetic energy. The relationship between the kinetic energy spectrum and the vorticity spectrum, $V(\kappa)$:

$$V(\kappa) = \kappa^2 E(\kappa),$$

does not require the flow to be solenoidal, merely isotropic. So the drifter dispersion may reflect the surface kinetic energy spectra, regardless of surface divergence effects.

We wondered whether the non-conservation of the triangle areas at the earliest times was evidence of surface divergence effects. But this need not be true; such growth can also occur in a non-divergent flow if the particles experience random perturbations. Consider the random strain model of Kraichnan (1974). In this, the separation vector **D** between two particles evolves according to:

$$\frac{d}{dt} D_1 = pD_1, \quad \frac{d}{dt} D_2 = -pD_2 \tag{9}$$

where D_1 and D_2 are the separation components in the direction of the principal axes of the local rate of strain tensor, and p is a stationary random variable. This model yields exponential growth and contraction and moreover reproduces most of the statistical features of an enstrophy cascade (Bennett, 1984).

As we have seen, the drifters experience small scale (order 1 km) deflections (Fig. 12) due possibly to Ekman advection, windage effects or positioning errors. To incorporate these into the random strain model, we would append stationary noise terms to the RHS of both equations in (9). Then, under the same limit considered by Kraichnan (in which the decay time associated with the mean of p is much longer than the decorrelation time of p), the separations parallel to the strain axis would grow exponentially but the normal separations would grow diffusively (as time to the one-half power). Triangle areas would then likewise grow exponentially in time, and with an e-folding time consistent with that deduced from two particle dispersion. So areal growth need not reflect surface divergence.

The observation of exponential growth is probably the most significant finding in the present study. LaCasce and Bower (2000) also looked for this but did not find it. We have had two advantages in this regard: (1) we have much smaller initial pair separations (1 km rather than 10 km) and (2) the deformation radius is slightly larger in the Gulf of Mexico (45 km vs. 10–30 km). The result is a longer range of scales over which to observe such stretching.

With regards to the Gulf of Mexico, the most interesting observation may be of local turbulent straining. The Loop eddies are a well known feature here (Kutsenov *et al.,* 2002 and references therein). But our results suggest a spectral continuum of eddies, with eddies of a given scale affecting relative dispersion at the same scale.

Lastly, these results tell us something about the fate of tracers at the sea surface in the Gulf, for instance spilled oil. Exponential stretching is associated with the drawing out of tracer into long filaments. These filaments become narrower as they lengthen, until lateral mixing limits their collapse (Garrett, 1983). Such filamentation is very different than simple lateral diffusion because maximum concentrations and strong gradients are better preserved. Recognizing this, as well as the scales up to which exponential growth occurs, could well aid spill containment strategies.

Acknowledgments. We are grateful for suggestions from three anonymous reviewers and G. Boffetta. JHL thanks R. Weller and a SECNAV scholarship for support while at WHOI. CO was supported by the U.S. Minerals Management Service grant 136870029. We are grateful to P. Niiler and the M.M.S. for the SCULP data.

REFERENCES

Anikiev, V. V., O. V. Zaytsev, T. V. Zaytseva and V. V. Yarosh. 1985. Experimental investigation of the diffusion parameters in the ocean. Izv. Atmos. Ocean Phys., *21,* 931–934.

Aurell, E., G. Boffetta, A. Crisianti, G. Paladin and A. Vulpiani. 1997. Predictability in the large: an extension of the concept of Lyapunov exponent. J. Phys. A: Math. Gen., *30,* 1–26.

Babiano, A., C. Basdevant, P. LeRoy and R. Sadourny. 1990. Relative dispersion in two-dimensional turbulence. J. Fluid Mech., *214,* 535–557.

Batchelor, G. K. 1952a. Diffusion in a field of homogeneous turbulence, II; the relative motion of particles. Proc. Cambridge Philo. Soc., *48,* 345–362.

——1952b. The effect of homogeneous turbulence on material lines and surfaces. Proc. Roy. Soc., A, *213,* 349–366.

Bennett, A. F. 1984. Relative dispersion: local and nonlocal dynamics. J. Atmos. Sci., *41,* 1881–1886.

——1987. A Lagrangian analysis of turbulent diffusion. Rev. of Geophys., *25*(4), 799–822.

Boffetta, G. and I. M. Sokolov. 2002. Relative dispersion in fully developed turbulence: The Richardson's Law and intermittency corrections. Phys. Fluids, *14,* 3224–3232.

Brown, M. G. and K. B. Smith. 1990. Are SOFAR float trajectories chaotic? J. Phys. Oceanogr., *20,* 139–149.

Celani, A. and M. Vergassola, 2001. Statistical geometry in scalar turbulence. Phys. Rev. Lett., *86,* 424–427.

Chelton, D. B., R. A. deSzoeke, M. G. Schlax, K. El Naggar and N. Siwertz. 1998. Geographical variability of the first-baroclinic Rossby radius of deformation. J. Phys. Oceanogr., *28,* 433–460.

Davis, R. E. 1985. Drifter observations of coastal surface currents during CODE: the statistical and dynamical view. J. Geophys. Res., *90,* 4756–4772.

Er-el, J. and R. Peskin. 1981. Relative diffusion of constant-level balloons in the Southern hemisphere. J. Atmos. Sci., *38,* 2264–2274.

Falkovich, G., K. Gawedzki and M. Vergassola. 2001. Particles and fields in fluid turbulence. Rev. Mod. Phys., *73*(4), 913–975.

Garrett, C. 1983. On the initial streakiness of a dispersing tracer in two- and three-dimensional turbulence. Dyn. Atmos. Oceans, *7,* 265–277.

Kuznetsov, L., M. Toner, A. D. Kirwan, Jr., C. K. R. T. Jones, L. H. Kantha and J. Choi. 2002. The Loop Current and adjacent rings delineated by Lagrangian analysis of the near-surface flow. J. Mar. Res., *60,* 405–429.

Kraichnan, R. H. 1974. Convection of a passive scalar by a quasi-uniform random straining field. J. Fluid Mech., *64,* 737–762.

LaCasce, J. H. 2000. Floats and f/H. J. Mar. Res., *58,* 61–95.

LaCasce, J. H. and A. Bower. 2000. Relative dispersion in the subsurface North Atlantic. J. Mar. Res., *58,* 863–894.

Lacorata, G., E. Aurell and A. Vulpiani. 2001. Drifter dispersion in the Adriatic Sea: Lagrangian data and chaotic model. Ann. Geophys., *19,* 121–129.

Ledwell, J. R., A. J. Watson and C. S. Law. 1998. Mixing of a tracer in the pycnocline. J. Geophys. Res., *103,* 21499–21529.

Lichtenberg, A. J. and M. A. Lieberman. 1992. Regular and Chaotic Dynamics, Springer-Verlag, 655 pp.

Molinari, R. and A. D. Kirwan, Jr. 1975. Calculations of differential kinematic properties from Lagrangian observations in the Western Caribbean Sea. J. Phys. Oceanogr., *5,* 483–491.

Morel, P. and M. Larcheveque. 1974. Relative dispersion of constant-level balloons in the 200 mb general circulation. J. Atmos. Sci., *31,* 2189–2196.

Obhukov, A. M. 1941. Energy distribution in the spectrum of turbulent flow. Izv. Akad. Nauk. SSR, Ser. Geogr. Geofiz., *5,* 453–466.

Ohlmann, J. C. and P. P. Niiler. 2003. Ocean circulation over the continental shelf in the northern Gulf of Mexico. Prog. Oceanography (in prep).

Okubo, A. 1971. Oceanic diffusion diagrams. Deep-Sea Res., *18,* 789–802.

Okubo, A. and C. Ebbesmeyer. 1976. Determination of vorticity, divergence and deformation rates from analysis of drogue observations. Deep-Sea Res., *23,* 349–352.

Ottino, J. M. 1989. The Kinematics of Mixing, Camb. Univ. Press, 378 pp.

Poulain, P. M. and P. P. Niiler. 1989. Statistical analysis of the surface circulation in the California current system using satellite-tracked drifters. J. Phys. Oceanogr., *19,* 1588–1603.

Pumir, A. 1998. Structure of the three-point correlation function of passive scalar in the presence of a mean gradient. Phys. Rev. E, *57,* 2914–2929.

Richardson, L. F. 1926. Atmospheric diffusion on a distance-neighbour graph. Proc. R. Soc. London, Ser. A, *110,* 709–737.

Richardson, L. F. and H. Stommel. 1948. Note on eddy diffusion in the sea. J. Meteorol., *5*(5), 38–40.

Schumacher, J. and B. Eckhardt. 2002. Clustering dynamics of Lagrangian tracers in free-surface flows. Phys. Rev. E, *66,* 017303.

Shepherd, T. G., J. N. Koshyk and K. Ngan. 2000. On the nature of large-scale mixing in the stratosphere and mesosphere. J. Geophys. Res., *105,* 12433–12446.

Shraiman, B. I. and E. D. Siggia. 2000. Scalar turbulence. Nature, *405,* 639–646.

Sullivan, P. J. 1971. Some data on the distance-neighbour function for relative diffusion. J. Fluid Mech., *47,* 601–607.

Sundermeyer, M. A. and J. F. Price. 1998. Lateral mixing and the North Atlantic tracer release experiment: Observations and numerical simulations of Lagrangian particles and a passive tracer. J. Geophys. Res., *103,* 21,481–21,497.

Townsend, A. A. 1951. The diffusion of heat spots in homogeneous turbulence. Proc. Roy. Soc., A, *224,* 418–430.

Warhaft, Z. 2000. Passive scalars in turbulent flows. Ann. Rev. Fluid Mech., *32,* 203–240.

Received: *10 October, 2002;* revised: *21 April, 2003.*